THE JOURNAL OF PHYSICAL CHEMISTRY C

ARTICLE

pubs.acs.org/JPCC

Covalent State and the Electronic and Transport Properties of $CaCu_3Ni_4O_{12}$: A First-Principles Study

Shuhui Lv,[†,‡] Xiaojuan Liu,[*,†] Hongping Li,[†,‡] Deming Han,[†] and Jian Meng[*,†]

[†]State Key Laboratory of Rare Earth Resource Utilization, Changchun Institute of Applied Chemistry, Chinese Academy of Sciences, Changchun 130022, P. R. China

[‡]Graduate School, Chinese Academy of Sciences, Beijing 100049, P. R. China

ABSTRACT: The structure stability and physical properties of $CaCu_3Ni_4O_{12}$ have been studied by first-principles calculations. It shows that $CaCu_3Ni_4O_{12}$ is stable both thermodynamically and mechanically. The electronic structure analysis reveals that the Cu covalence is formally +3 and that the Cu ions have the d^9L configuration (L: an O 2p hole) that corresponds to the Zhang−Rice singlet state. It is predicted to be a ferromagnetic half-metal, comparable to the metallic character of its isostructural compound of $CaCu_3Co_4O_{12}$. Electron correlation plays a vital role in stabilizing the half-metallic property of $CaCu_3Ni_4O_{12}$. The Fermi level shifts toward the middle of the minority-spin gap with the increase of U, demonstrating its stability of the half metallicity against structural distortion. Moreover, it is found that O atoms carry unusual large magnetic moments due to the enhanced exchange splitting with the increase of U. All the predicted properties for $CaCu_3Ni_4O_{12}$ are comparable with the corresponding existing compound $CaCu_3Co_4O_{12}$. Therefore, interesting physical properties are also expected from $CaCu_3Ni_4O_{12}$.

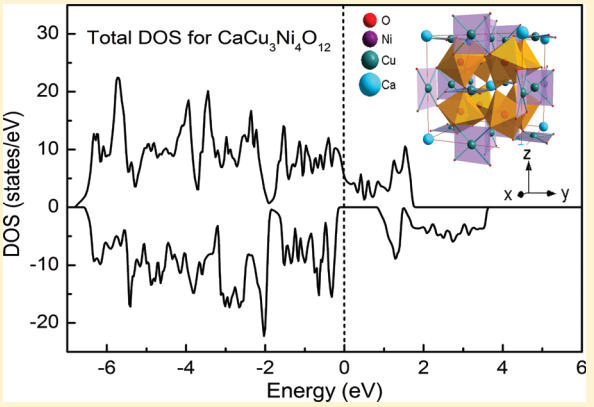

1. INTRODUCTION

The half-metallic ferromagnet could be useful for spintronics due to its 100% spin polarization at the Fermi level.[1−4] This character can avoid the spin-related scattering processes that should exist otherwise, which is crucial in practical application. The half-metallic ferromagnetism has been found in Heusler alloys, transition-metal oxides, binary transition-metal pnictides and chalcogenides, and even in graphene nanoribbons. It is therefore significant to find more useful half-metallic ferromagnets.

Electron correlation plays a significant role in understanding the electronic and magnetic properties in transition-metal materials. Since the local density approximation (LDA) (or generalized gradient approximation (GGA)) often results in an incorrect description of the magnetic ground state due to its underestimation of the Coulomb repulsion,[5−7] it is necessary to take into account the on-site Coulomb repulsion. Especially, it has been pointed out that the on-site electron correlation plays an important role in the description of the half-metallic property in Co_2MnSi and Co_2FeSi.[8] Also, GGA + U calculations correctly obtained the half-metallic ground state in Sr_2CoO_4, opposing the GGA results.[9] And the on-site correlation is found to be important to reproduce the experimentally observed high degree of transport spin polarization in $CeMnNi_4$.[10]

Recently, the strong correlated system $ACu_3B_4O_{12}$ (A is a divalent and/or trivalent cation and B is a transition-metal element) has attracted much attention as a result of its interesting and unexpected properties. After $CaCu_3Mn_4O_{12}$ is first discovered to be a semiconducting colossal magnetoresistance material with high Curie temperature as much as 355 K,[11] half-metallic property is successively predicted theoretically in this series of compounds with the atomic number of transition metal increase from V to Fe based on $CaCu_3Mn_4O_{12}$. For example, $LaCu_3Mn_4O_{12}$, $CaCu_3V_4O_{12}$, and $CaCu_3Cr_4O_{12}$ are then theoretically predicted to be half-metallic.[12−14] Subsequently, $BiCu_3Mn_4O_{12}$ is experimentally found to be half-metallic due to the same mechanism in $LaCu_3Mn_4O_{12}$,[15] and then $CaCu_3Fe_4O_{12}$ is found to be a half-metal at higher temperature although it is a Fe-sites-large-disproportionated ferrimagnetic (FiM) semiconductor at low temperature.[16] In all the above compounds where B 3d orbitals are less than half-filled (d^n, $0 < n < 5$), the valence of Cu is +2 and the coupling of Cu−B is FiM, whereas those of Cu−Cu and B−B are ferromagnetic (FM). However, for B being Co where Co 3d orbitals are half-filled, it is suggested to be ferromagnetic metallic (not half-metallic) due to the low-spin state of Co with electronic configuration of $t_{2g}^5e_g^0$ and Cu^{3+} with d^9L configuration.[17,18]

Following the studies above, it should be very interesting and natural to carry out investigations on the hypothetical compound

Received: September 6, 2010
Revised: December 8, 2010
Published: January 7, 2011

$CaCu_3Ni_4O_{12}$ where Ni 3d orbitals are more than half-filled. First structural stability is theoretically verified. Then the covalent state of Cu is determined to be +3 and has d^9L configuration. Last, the electronic and transport properties of $CaCu_3Ni_4O_{12}$ are presented. Particularly, the electron correlation effect on its electronic and transport properties especially on its half-metallic property is thoroughly investigated.

2. COMPUTATIONAL METHODS

Geometry optimization, formation enthalpy (ΔE_H), and elastic constant calculations were performed within the CASTEP code.[19] The Vanderbilt ultrasoft pseudopotential,[20] which describes the interaction of valence electrons with ions, was used with the cutoff energy of 340 eV. The exchange and correlation functional were treated by the generalized gradient approximation by Perdew, Burke, and Ernzerhof (GGA-PBE).[21]

The electronic and magnetic properties were performed using the full-potential linearized augmented plane wave (FPLAPW) plus local orbital method (LO),[22,23] as implemented in the WIEN2K code.[24] The muffin-tin radii (RMT) used are 2.50, 1.87, 1.93, and 1.66 bohrs for Ca, Cu, Ni, and O, respectively. The spherical-harmonic expansion of the potential was performed up to l_{max} = 10. The plane wave expansion cutoffs are 7.0 for expanding the wave function ($R_{MT}K_{max}$) and 14 for expanding the densities and potentials (G_{max}). 1000k points were used in the whole Brillouin zone. The Brillouin zone integration is carried out with a modified tetrahedron method.[25] For the exchange-correlation energy functional, the GGA-PBE was also employed.[21] The self-consistent calculations were considered to be converged when the energy convergence is less than 10^{-5} Ry. In addition, to improve the description of transition-metal elements, electron−electron Coulomb interactions for Cu and Ni are considered. We used the approach of Dudarev et al.[26] to describe the electron correlation with an effective Hubbard parameter $U_{eff} = U-J$ (U and J are the Hubbard parameter and the exchange interaction, respectively). For simplicity, we use U to represent U_{eff} in the following.

3. RESULTS AND DISCUSSION

Crystal Structure. Geometry optimization of $CaCu_3Ni_4O_{12}$ was performed based on the crystal structure of $CaCu_3Mn_4O_{12}$ with $Im\bar{3}$ space group by both nonspin polarization (NSP) and spin polarization (SP) methods. The results indicate that the total energy of SP is lower by 21 meV per formula unit than that of NSP, suggesting that the SP state is the ground state of $CaCu_3Ni_4O_{12}$. Therefore, we only show the results from the SP calculation below. The optimized crystal structure of $CaCu_3Ni_4O_{12}$ is shown in Figure 1, and the optimized lattice parameters, atomic positions, and selected bond lengths and angels are given in Table 1. It is seen that the structure of $CaCu_3Ni_4O_{12}$ is cubic with coordination numbers of 12, 6, and 4 for Ca, Ni, and Cu, respectively. All the Ni−O bond distances are the same (1.941 Å) in NiO_6 octahedra, comparable to the corresponding Co−O bond distances of 1.901 Å in $CaCu_3Co_4O_{12}$.[27] The tilting of the NiO_6 octahedron destroys the 4-fold axis in an ideal octahedron. Thus, there is only one 3-fold axis going through each NiO_6 octahedron. Therefore, the Ni 3d orbitals cannot be represented by the standard t_{2g}/e_g representations as in an ideal octahedron. The $\bar{3}$ symmetry at Ni sites splits the five 3d orbitals to $3z^2 - r^2$, $\{x^2 - y^2, xy\}$, and $\{xz, yz\}$. Also, the corner-sharing

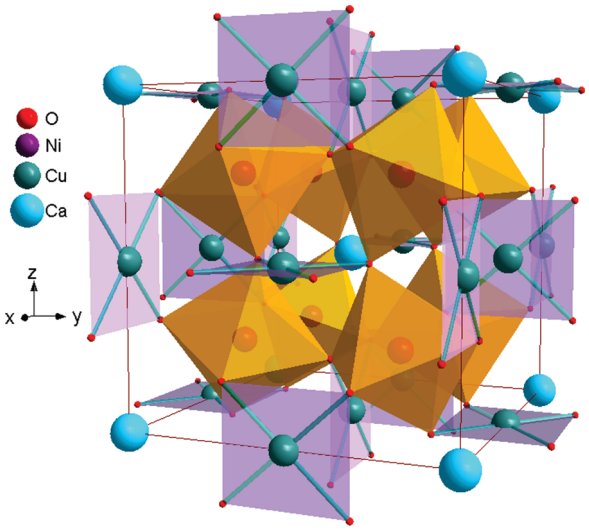

Figure 1. Crystal structure of $CaCu_3Ni_4O_{12}$.

Table 1. Optimized Crystallographic Data of Spin-Polarized $CaCu_3Ni_4O_{12}$ with $Im\bar{3}$ Symmetry and Selected Bond Lengths and Angles

atom	x	y	z
Ca	0.00	0.00	0.00
Cu	0.00	0.00	0.50
Ni	0.25	0.25	0.25
O	0.3094	0.1729	0.00
SG: $Im\bar{3}$, $a = b = c = 7.23683$ Å, $\alpha = \beta = \gamma = 90°$			
Ni−O/Å	1.941 × 6	O−Cu−O	95.56°
Cu−O/Å	1.863 × 4		84.44°
	2.739 × 4	O−Ni−O	89.87°
	3.258 × 4		90.13°
		Ni−O−Ni	137.47°
		Cu−O−Ni	110.92°

NiO_6 octahedra in this structure are heavily tilted, giving rise to the Ni−O−Ni bond angle of 137.47° from an ideal 180°, which is comparable with the corresponding Co−O−Co angles of 139.36° in $CaCu_3Co_4O_{12}$.[27] Distortion is also found in the CuO_4 unit. The symmetry of CuO_4 is lowered from D_{4h} symmetry in an ideal planar square to pseudo-D_{4h} symmetry with a planar rectangular shape, as seen from Figure 1. The five 3d orbitals are completely split by the mmm symmetry at the Cu sites.

Thermodynamic and Mechanical Stabilities. First, the formation enthalpy (ΔE_H) was calculated to investigate the thermodynamic stability of $CaCu_3Ni_4O_{12}$. The following two reactions are considered

$$CaO + 3CuO + 4NiO + 2O_2 = CaCu_3Ni_4O_{12} \quad (1)$$

$$CaCO_3 + 3CuO + 4NiO + 2O_2 = CaCu_3Ni_4O_{12} + CO_2 \quad (2)$$

The ΔE_H of $CaCu_3Ni_4O_{12}$ was estimated by the total energy difference after structural relaxation of the sum of products minus those of the reactants. For the reactants, the space groups of $Fm\bar{3}m$ for CaO, $R\bar{3}c$ for $CaCO_3$, $C2/c$ for CuO, $Fm\bar{3}c$ for NiO, $C2/m$ for O_2 (solid molecule), and $Pa\bar{3}$ for CO_2 (solid molecule)

dx.doi.org/10.1021/jp108482c |J. Phys. Chem. C 2011, 115, 2366–2370

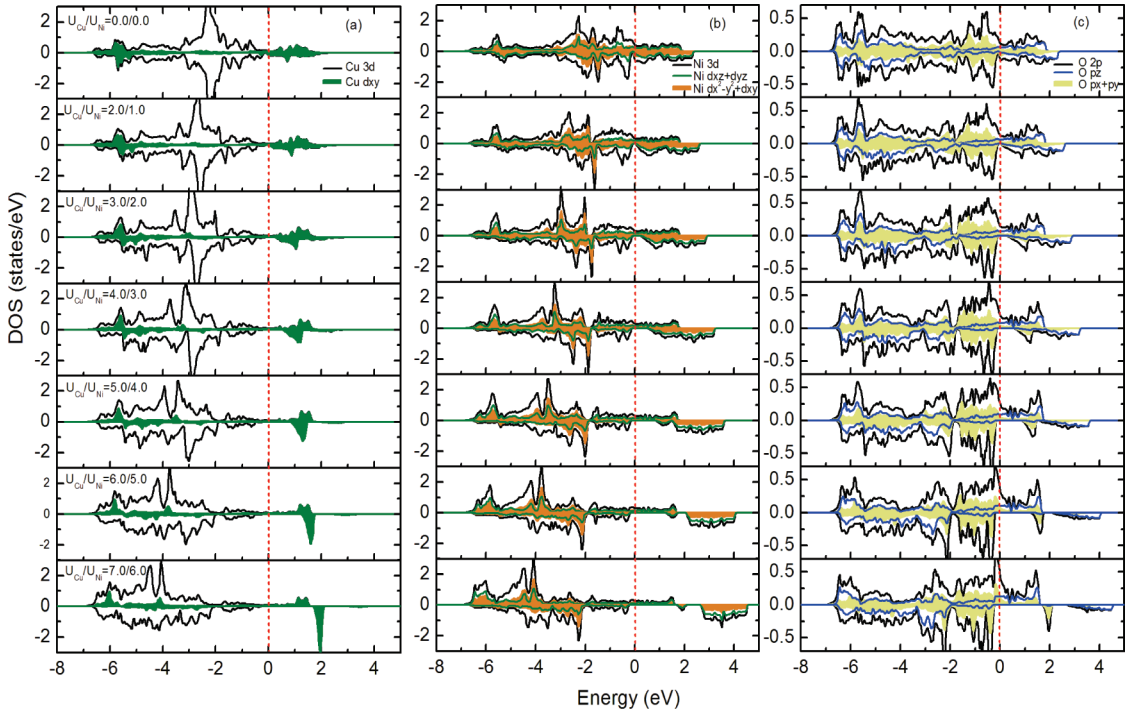

Figure 2. PDOS changes of (a) Cu 3d, (b) Ni 3d, and (c) O 2p in $CaCu_3Ni_4O_{12}$ with the increase in values of U_{Cu} and U_{Ni} (in eV). The vertical dotted line denotes the Fermi level.

are adopted. The calculated results give ΔE_H to be −5.81 and −6.58 eV for reactions 1 and 2, respectively. The negative values of ΔE_H suggest that the assumed reactions can proceed, and $CaCu_3Ni_4O_{12}$ is thermodynamically stable. Notice that the value of ΔE_H for $CaCu_3Ni_4O_{12}$ is much lower than that of $CaCu_3Fe_4O_{12}$,[28] which implies that $CaCu_3Ni_4O_{12}$ could be synthesized more easily.

Since the accurate calculation of elasticity is essential for understanding the macroscopic mechanical properties of solids, the elastic coefficients are determined to study the mechanical stability of $CaCu_3Ni_4O_{12}$. The calculated elastic constants are C_{11} = 269 GPa, C_{44} = 83 GPa, and C_{12} = 124 GPa. It is known that for cubic crystals its three independent elastic constants C_{11}, C_{44}, and C_{12} should satisfy the following criteria:[29] $C_{11} > 0$, $C_{44} > 0$, $C_{11} > |C_{12}|$, $(C_{11} + 2C_{12}) > 0$. Clearly, the calculated elastic constants satisfy the criteria, suggesting that $CaCu_3Ni_4O_{12}$ is mechanically stable.

Covalence States of Cu and Ni. The correct determination of covalent states of Cu and Ni is essentially basic to analyze the electronic and magnetic properties of $CaCu_3Ni_4O_{12}$. Thus, we first determine the Cu and Ni covalent states in $CaCu_3Ni_4O_{12}$. We calculated both FiM and FM configurations for Cu and Ni moments within GGA and GGA + U methods. For U = 0.0 eV, the FiM calculation converges to FM, indicating that FM is more stable than FiM configuration in $CaCu_3Ni_4O_{12}$. Calculation by forcing the spin alignment of Cu and Ni in the reverse direction shows that FiM configuration is 21 meV per formula unit higher in energy than that of FM configuration. The calculated magnetic moments are 0.03 μ_B for Cu, 0.5 μ_B for Ni, and 0.03 μ_B for O with a total net magnetic moment of 2.67 μ_B. The comparatively small magnetic moments on Cu indicate that the covalent state of Cu deviates from +2. Partial density of states (PDOS) of Cu in Figure 2(a) shows that spin-up and spin-down channels of the Cu d_{xy} orbital mix together, being partially occupied under the Fermi level and unoccupied above the Fermi level. Suppose the Cu ion is a paramagnetic ion; then, there are only Ni magnetic ions, like the case in $LaCu_3Fe_4O_{12}$[30] and $BiCu_3Fe_3O_{12}$[31] in which Cu is +3 and Fe−Fe antiferromagnetically coupled in low temperature. We suspect this kind of magnetic coupling may occur in $CaCu_3Ni_4O_{12}$, and thus, we initialize Ni−Ni antiferromagnetically coupled and Cu as a paramagnetic ion. Calculated magnetic moments are 0.028 μ_B and 0.44 μ_B for Cu and Ni, respectively. Moreover, the initialized AFM Ni−Ni converged to the FM state. In contrast, we notice that in $CaCu_3Ti_4O_{12}$ Cu−Cu is antiferromagnetically coupled by superexchange interaction by way of Cu−O−Ti−O−Cu.[32] Within $CaCu_3Ni_4O_{12}$, if Cu is +2, then Ni should be +4, resulting in $3d^6$ configuration. Provided that Ni is in the low spin state, Ni can also provide d orbitals to mediate the Cu−Cu antiferromagnetic coupling. On the basis of this assumption, we performed further calculations on the magnetic state of Cu−Cu antiferromagnetically coupled. Similarly, it is found that the AFM Cu−Cu also converges to the FM state with the magnetic moments of Cu and Ni being 0.001 μ_B and 0.360 μ_B, respectively. These facts demonstrate that in $CaCu_3Ni_4O_{12}$ Cu−Cu, Ni−Ni, and Cu−Ni are all prone to ferromagnetic coupling. Actually, the ferromagnetically coupled Cu−Co is also obtained in $CaCu_3Co_4O_{12}$ where the Co 3d orbitals are more than half-filled.[17] The small calculated magnetic moments and the PDOS indicate that Cu is +3; however, it should be d^9L configuration that corresponds to the Zhang−Rice singlet state since Cu still participates in magnetic interactions according to all the calculations above, and this results in the covalent state of Ni being +3.25. These similar results have already been experimentally found in $CaCu_3Co_4O_{12}$.[18]

Electronic Correlation Effect on Electronic Transport Property. Furthermore, GGA + U calculations were conducted to investigate how the magnetic and electronic structures depend on electron correlation. Because the parameter U is system-dependent

dx.doi.org/10.1021/jp108482c |J. Phys. Chem. C 2011, 115, 2366–2370

Table 2. Calculated Total Magnetic Moments M_{total} per Formula Unit and Magnetic Moments of Cu (M_{Cu}), Ni (M_{Ni}), and O (M_O) ions (in μ_B) and the Spin Gap (in eV) in the Minority-Spin Channel (E_{gap}) in $CaCu_3Ni_4O_{12}$ Obtained by GGA + U with U from (0.0, 0.0) eV to (7.0, 6.0) eV for (U_{Cu}, U_{Ni})

U_{Cu}	0.0	2.0	3.0	4.0	5.0	6.0	7.0
U_{Ni}	0.0	1.0	2.0	3.0	4.0	5.0	6.0
M_{total}	2.67	3.00	3.00	3.00	3.00	3.00	3.00
M_{Cu}	0.03	0.06	0.08	0.09	0.11	0.19	0.28
M_{Ni}	0.50	0.65	0.77	0.89	1.01	1.13	1.23
M_O	0.04	0.01	−0.03	−0.07	−0.11	−0.16	−0.21
E_{gap}	0.00	0.03	0.22	0.51	0.87	1.31	1.82

and its variation with its environment is not well understood, a series of U values were chosen in this study. Since the electronic correlations gradually strengthen as the atomic number of transition metal increases from Ti to Cu,[33] we consider different U values for Cu and Ni, where U_{Cu} is from 2.0 to 7.0 eV and U_{Ni} from 1.0 to 6.0 eV. The calculated results are listed in Table 2. Similar to that of GGA, the initializing FiM state also converges to the FM state within GGA + U calculations. This further demonstrates the strong ferromagnetic coupling between Cu and Ni ions, and the FM ground state is robust to the electron correlation. The total density of states (TDOS) near the Fermi level from GGA + U calculations is present in Figure 3 along with the result of GGA for comparison. From Figure 3, it is clear that half-metallic behavior is obtained as long as U is taken into account. Even a small value of U, say U_{Cu}/U_{Ni} = 2.0/1.0 eV, is enough to open a gap in the minority spin channel, giving the half-metallic property. This indicates that the electronic structure is very sensitive to the electron correlation, which plays an important role in realizing the half-metallic feature in $CaCu_3Ni_4O_{12}$. Further, it is noted that the minority spin gap increases with the increase of U (see Table 1), such as from 0.03 eV for U_{Cu}/U_{Ni} = 2.0/1.0 to 1.82 eV for U_{Cu}/U_{Ni} = 7.0/6.0 eV. More importantly, the Fermi level is shifted toward the middle of the minority-spin gap. This is appealing since, from the practical application point of view, the position of E_F in the half-metallic gap is an important factor in determining the stability of half-metallicity against structural distortion. Therefore, it is claimed that electronic correlation should help to control the position of E_F to the center of the half-metallic gap. This statements call for future experimental studies of $CaCu_3Ni_4O_{12}$, such as by using photoemission spectroscopy and soft X-ray absorption spectroscopy, which can provide valuable information on the valence states and electronic structures.

Electronic Correlation Effect on Electronic Structure. To explain why electronic correlation in $CaCu_3Ni_4O_{12}$ plays such a crucial role in determining the electronic structure of $CaCu_3Ni_4O_{12}$, we have shown in Figure 2 (a, b, and c) the partial density of states (PDOS) evaluated at various U values of Cu 3d, Ni 3d, and O 2p states, respectively. When U = 0.0 eV, for both Cu and Ni, one can clearly see that there exist strong hybridizations of Cu 3d, Ni 3d, and O 2p states. The Cu 3d orbitals are almost completely occupied in both spin channels, despite the small DOS appearing in the d_{xy} orbital above the Fermi level which can be considered to be induced from the hybridization with Ni 3d and O 2p states. Ni 3d orbitals, which are split into d_{z^2}, $\{d_{x^2-y^2}, d_{xy}\}$, and $\{d_{xz}, d_{yz}\}$, are substantially delocalized with a wide energy range. The Ni dz^2 is doubly occupied which allows a considerable reduction of the intra-atomic Coulomb repulsion,[34,35] and the two doubly degenerate orbitals, $\{d_{x^2-y^2}, d_{xy}\}$ and $\{d_{xz}, d_{yz}\}$, are partially occupied in both spin channels and, combined with O 2p states, contribute mainly to DOS at the Fermi energy. As U is considered, one can notice that both the Cu 3d and Ni 3d states are shifted to the lower energy region, with the half-metallic gap increased remarkably from 0.03 eV for U_{Cu}/U_{Ni} = 2.0/1.0 to 1.62 eV for U_{Cu}/U_{Ni} = 7.0/6.0 eV. Note that the increase in the gap value is accompanied by the enhancement of the spin magnetic moment for Cu, Ni, and O (see Table 2). However, the calculated total net magnetic moment for each formula unit remains nearly unchanged with the increase of U, i.e., 3.00 μ_B (Table 2). This integer value of total magnetic moment is a typical character of half-metallic materials.

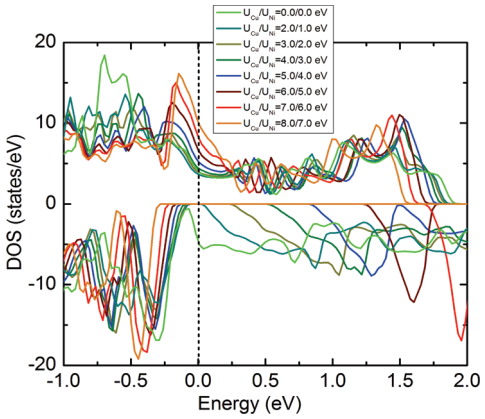

Figure 3. Spin-resolved total density of states (TDOS) for $CaCu_3Ni_4O_{12}$ with different U_{Cu} and U_{Ni} (in eV) values obtained by the GGA + U method. The vertical dotted line denotes the Fermi level.

It is interesting to note that, as listed in Table 2, in $CaCu_3Ni_4O_{12}$ the O atoms carry large magnetic moments when U is considered. For example, when U_{Cu}/U_{Ni} is 7.0/6.0 eV, the magnetic moments at O reaches −0.21 μ_B, comparable with the absolute value in the literature.[36,37] Figure 2(c) shows that the p_z orbital of O lies in the energy region from −7.0 to −2.0 eV, strongly overlapping with 3d states of Cu and Ni. The exchange splitting of the p_z states of O is very small, thus making a small contribution to the magnetic moment. For the p_x and p_y orbitals, they are almost degenerated with a large density of states distributed from −1.0 to 0.0 eV. As U is not included, sizable distributions from p_x and p_y states of O are seen at the Fermi energy in both the spin channels, indicating that there is no exchange splitting of p_x and p_y orbitals. When U is considered, a gap is opened and increases with increasing U in the spin-down channel. However, the states in the spin-up channel are obviously higher in energy than those in the spin-down channel and cross the Fermi level. This clearly suggests that there exits rather strongly exchange splitting in p_x and p_y bands, and the magnetic moment at O is carried mainly by the degenerated p_x and p_y states. We noticed that the p_x and p_y orbitals split is closely related with the splitting of the Cu d_{xy} orbital. This indicates that the O 2p hole is trapped by the Cu sites. A photoemission study will provide the experimental confirmation in the future, and this result is also consistent with the magnetic coupling analysis that the Cu 3d component can be coupled with the Ni 3d band via the O 2p component.

dx.doi.org/10.1021/jp108482c |J. Phys. Chem. C 2011, 115, 2366–2370

4. CONCLUSIONS

In summary, $CaCu_3Ni_4O_{12}$ is studied by density functional theory within both GGA and GGA + U methods. The calculated results indicate that $CaCu_3Ni_4O_{12}$ is stable both thermodynamically and mechanically. The total energy calculation results suggest that, similar to the ferromagnetic $CaCu_3Co_4O_{12}$, Cu−Ni is also ferromagnetically coupled within $CaCu_3Ni_4O_{12}$. The covalent state of Cu and Ni $CaCu_3Ni_4O_{12}$ is very similar to the case in $CaCu_3Co_4O_{12}$, namely, Cu is +3 with d^9L configuration (L: O 2p hole) and Ni is +3.25. Electronic structure analyses show that $CaCu_3Ni_4O_{12}$ is a half-metal, and electron correlation plays an important role in determining the half-metallic property. The enhanced exchange splitting of p_x and p_y orbitals of O due to electronic correlation makes O atoms carry unusual large magnetic moments, and the splitting is found to be consistent with results of the +3 covalent state of Cu with d^9L configuration and the ferromagnetic interaction between Cu and Ni.

AUTHOR INFORMATION

Corresponding Author

*E-mail: jmeng@ciac.jl.cn and lxjuan@ciac.jl.cn. Tel.: +86-431-85262030; +86-431-85262415. Fax: +86-431-85698041.

ACKNOWLEDGMENT

This work was supported by the National Natural Science Foundation of China through Grants Nos. 20831004, 20921002, and 21071141.

REFERENCES

(1) Wolf, S. A.; Awschalom, D. D.; Buhrman, R. A.; Daughton, J. M.; von Molnar, S.; Roukes, M. L.; Chtchelkanova, A. Y.; Treger, D. M. *Science* **2001**, *294*, 1488.
(2) Pickett, W. E.; Moodera, J. S. *Phys. Today* **2001**, *54*, 39.
(3) de Groot, R. A.; Mueller, F. M.; van Engen, P. G.; Buschow, K. H. J. *Phys. Rev. Lett.* **1983**, *50*, 2024.
(4) Kübler, J. *Phys. Rev. B* **2003**, *67*, 220403(R).
(5) Terakura, K.; Oguchi, T.; Williams, A. R.; Kübler, J. *Phys. Rev. B* **1984**, *30*, 4734.
(6) Anisimov, V. I.; Zaanen, J.; Andersen, O. K. *Phys. Rev. B* **1991**, *44*, 943.
(7) Miura, K.; Terakura, K. *Phys. Rev. B* **2001**, *63*, 104402.
(8) Candpal, H. C.; Fecher, G. H.; Felser, C.; Schönhense, G. *Phys. Rev. B* **2006**, *73*, 094422.
(9) Pandey, S. K. *Phys. Rev. B* **2010**, *81*, 035114.
(10) Bahramy, M. S.; Murugan, P.; Das, G. P.; Kawazoe, Y. *Phys. Rev. B* **2010**, *81*, 165114.
(11) Zeng, Z.; Greenblatt, M.; Subramanian, M. A.; Croft, M. *Phys. Rev. Lett.* **1999**, *82*, 3164.
(12) Liu, X. J.; Xiang, H. P.; Cai, P.; Hao, X. F.; Wu, Z. J.; Meng, J. *J. Mater. Chem.* **2006**, *16*, 4243.
(13) Xiang, H. P.; Wu, Z. J. *Inorg. Chem.* **2008**, *47*, 2706.
(14) Xiang, H. P.; Liu, X. J.; Zhao, E. J.; Meng, J.; Wu, Z. J. *Inorg. Chem.* **2007**, *46*, 9575.
(15) Takata, K.; Yamada, I.; Azuma, M.; Takano, M.; Shimakawa, Y. *Phys. Rev. B* **2007**, *76*, 024429.
(16) Hao, X. F.; Xu, Y. H.; Gao, F. M.; Zhou, D. F.; Meng, J. *Phys. Rev. B* **2009**, *79*, 113101.
(17) Xiang, H. P.; Liu, X. J.; Meng, J.; Wu, Z. J. *J. Phys.: Condens. Matter* **2009**, *21*, 045501.
(18) Mizokawa, T.; Morita, Y.; Sudayama, T.; Takubo, K.; Yamada, I.; Azuma, M.; Takano, M.; Shimakawa, Y. *Phys. Rev. B* **2009**, *80*, 125105.
(19) Segall, M. D.; Lindan, P. L. D.; Probert, M. J.; Pickard, C. J.; Hasnip, P. J.; Clark, S. J.; Payne, M. C. J. *J. Phys.: Condens. Matter* **2002**, *14*, 2717.
(20) Vanderbilt, D. *Phys. Rev. B* **1990**, *41*, 7892.
(21) Perdew, J. P.; Burke, K.; Ernzerhof, M. *Phys. Rev. Lett.* **1996**, *77*, 3865.
(22) Singh, D. J.; Nordstrom, L. *Planewaves, Pseudopotentials and the LAPW Method*, 2nd ed.; Springer: Berlin, 2006.
(23) Singh, D. *Phys. Rev. B* **1991**, *43*, 6388.
(24) Blaha, P.; Schwarz, K.; Madsen, G. K. H.; Kvasnicka, D.; Luitz, J. *WIEN2K, an augmented plane wave+local orbitals program for calculating crystal properties*; Karlheinz Schawarz, Technische Universitat Wien: Vienna, 2001.
(25) Blöchl, P. E. *Phys. Rev. B* **1994**, *50*, 17953.
(26) Dudarev, S. L.; Botton, G. A.; Savrasov, S. Y.; Humphreys, C. J.; Sutton, A. P. *Phys. Rev. B* **1998**, *57*, 1505.
(27) Yamada, I.; Ishiwata, S.; Terasaki, I.; Azuma, M.; Shimakawa, Y.; Takano, M. *Chem. Mater.* **2010**, *22*, 5328.
(28) Xiang, H. P.; Liu, X. J.; Zhao, E. J.; Meng, J.; Wu, Z. J. *Appl. Phys. Lett.* **2007**, *91*, 011903.
(29) Nye, J. F. *Physical Properties of Crystals*; Oxford University Press: Oxford, 1985.
(30) Long, Y. W.; Hayashi, N.; Saito, T.; Azuma, M.; Muranaka, S.; Shimakawa, Y. *Nature (London)* **2009**, *458*, 60.
(31) Long, Y. W.; Saito, T.; Tohyama, T.; Oka, K.; Azuma, M.; Shimakawa, Y. *Inorg. Chem.* **2009**, *48*, 8489.
(32) Shiraki, H.; Saito, T.; Yamada, T.; Tsujimoto, M.; Azuma, M.; Kurata, H.; Isoda, S.; Takano, M.; Shimakawa, Y. *Phys. Rev. B* **2007**, *76*, 140403(R).
(33) Solovyev, I.; Hamada, N.; Terakura, K. *Phys. Rev. B* **1996**, *53*, 7158.
(34) Xiang, H. J.; Wei, S.-H.; Whangbo, M.-H. *Phys. Rev. Lett.* **2008**, *100*, 167207.
(35) Pruneda, J. M.; Íñiguez, J.; Canadell, E.; Kageyama, H.; Takano, M. *Phys. Rev. B* **2008**, *78*, 115101.
(36) Weht, R.; Pickett, W. E. *Phys. Rev. Lett.* **1998**, *81*, 2502.
(37) Wan, X. G.; Kohno, M.; Hu, X. *Phys. Rev. Lett.* **2005**, *95*, 146602.